Istraživanja i projektovanja za privredu
ISSN 1451-4117
DOI:10.5937/jaes0-40078
www.engineeringscience.rs

iipp publishing

Journal of Applied Engineering Science
Vol. 21, No. 1, 2023
Original Scientific Paper
Paper number: 21(2023)1, 1069, 253-262

SIMULATION OF FLOW THROUGH AN EQUISPACED IN-LINE CYLINDER IN OPEN CHANNELS

Sanaa A. Talab Al-Osmy, Shaymaa A.M. Al-Hashimi, Saad Mulahasan, Sabah H. Fartosy*

Water Resources Engineering Department, College of Engineering, Mustansiriyah University
** dr.sabah77@uomustansiriyah.edu.iq*

In this work, a numerical simulation using Computation Fluid Dynamics technique was used to investigate the flow properties and turbulence characteristics through flow of one-line cylinder in an open channel with uniform flow conditions. A two-dimensional turbulence model was applied using ANSYS. Flow properties were investigated against varying cylinder diameters that forms a one-line cylinder physical model and varying flow rates. Three cylinders diameters D were used (5.0 cm, 2.5 cm and 1.25 cm) and located at 12.5 cm apart along the flume centre-line. Spatial distributions of mean-stream-wise velocity, pressure, turbulent kinetic energy, and eddy viscosity were estimated. Results showed symmetrical distribution of flow velocity, turbulence eddy, and turbulent kinetic energy along the one-line cylinder for the largest cylinder diameter. Vortex shedding patterns were well predicted by the numerical simulation behind the cylinders. Different configurations of vortices distribution behind the cylinders were recorded for the diameters of 1.25 cm and 2.5 cm. The flow pattern difference between the largest diameter (5 cm) and the small diameters (2.5 cm and 1.25 cm) was leaded to the strong overlap for the vortices in the wake for the lined cylinders with the large diameter in comparison to the other diameters. Consequently, this study is investigated the different diameter sizes of a one-line cylinder with the same spacing between them on the flow pattern along the channel.

Keywords: simulation, one-line cylinders, ANSYS, turbulent flow, vortex patterns

1 INTRODUCTION

The flow through a one-line piercing vegetation is an important and remarkably complex flow. This vegetation arrangement can be observed on the bank of rivers and streams; may be trees or bushes. When placing more than one circular cylinder within the fluid flow, an alteration in the flow patterns is implemented. According to the literature; the flow in presence of a circular cylinder is well known and investigated by many researchers [1-3] two cylinders in tandem aligned with the flow directions has been extensively explained and discussed in many research papers [4-7]. Flow regimes pass an array of in-line cylinders are classified relative to the spacing ratio S/D between the cylinders, where D is the cylinder diameter and S is the space between cylinders. Zdravkovich [8] found that the value of S/D depends on the flow turbulence. Aiba and Yamazaki [9] and Igarashi and Suzuki [10] studied the effect of increasing the number of in-line cylinders on the flow patterns subjected to stronger turbulence. The results showed that the shedding patterns are affected if S/D is recognized. If four cylinders of equal diameters arranged in-line with the stream-wise flow, drag and pressure coefficients can be measured at each cylinder within the flow [8, 10, 11]. The flow through five in-line cylinders was investigated by [12]. The flow behavior of six in-line cylinders configuration with two values of spacing ratio are numerically investigated by [13, 14]. While, Liang et al. [15] numerically investigated the effect of S/D on the vortex shedding characteristics of laminar flow through a row of six cylindrical tubes. Flow through in-line circular cylinders along the channel were found in a number of research papers [2, 16, 17]. Mulahasan et al. [2] investigated the influence of in-line vegetation located along the main channel-floodplain in compound channels on discharge and span wise velocities. Yokojima et al. [17] investigated the flow through a one-line submerged cylinders. Drag coefficients of a one-line emergent or submerged vegetation elements are studied by researchers as [2, 16-20].

Several researchers [21-24] investigated the effect of the cylinder configuration on the flow pattern. Zhao et al. [21] made an investigation about vibration caused by the vortex due to four mounted separated and rigidly connected circular cylinders in one-line square configuration with a range of spacing ratio S/D from 1.5 to 4, Reynolds number of 150 and low mass ratio of 2.5. Lockard et al. [6] studied two identical centroids cylinders separated at the stream wise direction by 1.435 diameters. Salvador et al. [23] investigated the flow around two-in-tandem cylinders of diameter D=20mm and height H=50mm submerged in an open channel using large eddy simulation LES. The results showed that no vortex shedding occurs in the gap between the two cylinders for the spacing S = 2D. Hamed et al. [24] investigated the effect of spacing between two circular cylinders arranged in tandem in a water channel on the turbulent boundary using particle image velocimetry. The results showed that the flow characteristics are dependent on the spacing ratio. Keshavarzi et al. [25] investigated the flow structure interaction around bridge in-lined piers. Terrier et al. [19] worked on the examined the effect of flow resistance for in line vegetation located along the main channel-floodplain junction in compound channels to structure of flow and shear stress of boundary. Details measurements of the hydrodynamic behavior of in-line vegetation are scarce.

The main idea and goal of this study is to make an investigation of the flow patterns with a row of circular cylinders with three different set (diameter = D) placed along the centerline of a 0.3 m wide flume with the same distance

between them. A two-dimensional numerical approach was applied to elucidate the impacts of diameter size of the in line circular cylinders on the flow properties and turbulence characteristics along channel.

2 NUMERICAL AND EXPERIMENTAL MODEL

In this study, a numerical model was used to investigate how the patterns of flow are affected in the vicinity of the one-line cylinder at equispaced distances along the centerline of the flume length. For the experimental model, a laboratory flume of 10 m long, 30 cm wide and deep was used. An array of circular cylinders with equal diameters, such as (D = 1.25, 2.5, and 5 cm) located along the centerline of the flume at fixed distances (S = 12.5 cm).

2.1 Materials and methods

The flow past an array of circular cylinders was examined in a straight laboratory Perspex tilting flume under steady uniform flow conditions. The flume working section has 10 m length, 30 cm width and height. Three sizes of circular cylinders were examined of diameter 1.25, 2.5 and 5.0 cm (Fig. 1a) fixed at the bottom of the flume along the centerline of the working section at equispaced S = 12.5 cm as shown in (Fig. 1b) which can be named as case A, B and C depending on the diameter size. The height of the cylinders was selected to be of 10 cm and the slope of the flume was set to be 1/1000. During the experiments, a constant flow rate (Q = 3.0 l/sec) was measured using flow meter, while the water depth was measured by a point gauge with an accuracy ±0.1 mm. The upstream tank provided by honeycomb with hexagonal uniform holes which put at the inlet so as to straighten the flow through the working section in order to minimize the flow turbulence. Downstream the working section, a tailgate was located to control the water levels.

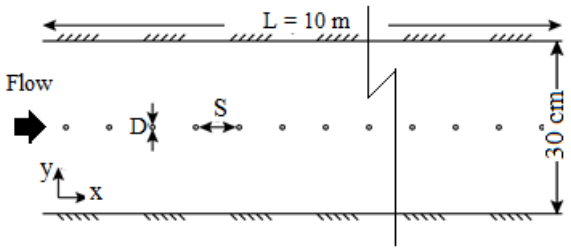

(a)

(b)

Figure1. a) a schematic diagram of the laboratory flume, b) a one-line circular cylinders at the flume centerline

2.2 ANSYS Fluent Numerical Model

In this research paper, ANSYS FLUENT version 19 was employed to investigate the flow patterns and turbulence through an array of in-line cylinders that was applied for running the numerical simulation. The Computation Fluid Dynamics (CFD) model has the capability of studying the problems of hydraulic flow with both compressible and incompressible fluids. The three-dimensional Reynold Averaged Navier stoke equations (RANS) are the governing equations of model [26] through applying the (finite volume method) on an unstructured grid, with closure models of turbulence K − ε [27] and K − ω [28]. The FLUENT are employed to solve 3D (RANS) equations of an incompressible flow which represented below:

$$\frac{\partial u_j}{\partial x_j} = 0 \tag{1}$$

$$\frac{\partial u_i}{\partial t} + u_j \frac{\partial u_i}{\partial x_j} = -\frac{1}{\rho}\frac{\partial p}{\partial x_i} + \frac{\partial}{\partial x_j}\left[(v + v_t)\frac{\partial u_i}{\partial x_j}\right] + g_i \tag{2}$$

Where,

i, j=1,2,3, u_i represents the components of mean velocity, x_i means the spatial vectorial component, v is the kinematic viscosity, v_t is the kinematic eddy viscosity, t is the time, ρ denoted the water density, p is the pressure, and g represents the gravity. In this study work, (K − ε) models applied to related the kinematic viscosity, v_t. The K − ε closure model gives a definition of the turbulent viscosity, v_t according to Equation [3]. Where, k is the turbulent kinetic energy, $c\mu$ is a constant equal to 0.09 and ε is the rate of energy dissipation as suggested by [29]

$$v_t = c_\mu \frac{k^2}{\epsilon} \tag{3}$$

The turbulent kinetic energy and dissipation are presented by transport equation shown in Equations (4) and (5), where σ_k, σ_ε, $c_{\varepsilon 1}$ and $c_{\varepsilon 2}$ are constant which have values equal to: 1, 1.3, 1.44 and 1.92, respectively, as suggested by [29]. The P_k turbulent production rate is shown in Equation [6].

$$\frac{\partial k}{\partial t} + u_j \frac{\partial k}{\partial x_j} = \frac{\partial}{\partial x_j}\left[\left(v + \frac{v_t}{\sigma_k}\right)\frac{\partial k}{\partial x_j}\right] + p_k - \epsilon \tag{4}$$

$$\frac{\partial \epsilon}{\partial t} + u_j \frac{\partial \epsilon}{\partial x_j} = \frac{\partial}{\partial x_j}\left[\left(v + \frac{v_t}{\sigma_\epsilon}\right)\frac{\partial \epsilon}{\partial x_j}\right] + c_{\epsilon 1}\frac{\epsilon}{k}p_k - c_{\epsilon 2}\frac{\epsilon^2}{k} \tag{5}$$

$$p_k = v_t \frac{\partial u_i}{\partial x_j}\left[\frac{\partial u_i}{\partial x_j} + \frac{\partial u_j}{\partial x_i}\right] \tag{6}$$

2.3 Meshing

Mesh is taken in consideration as one of the most important parameters that governed results of simulation. So, its process can change the time of operation according to change of the selected cells numbers. Different types of mesh accuracy have been tried for an accuracy by providing examined, providing the best time of computation with accurate results. The mesh size has been selected to satisfy the optimum cell size that get the best results. Two mesh planes have been taken into consideration with finer resolutions for both sides of the stem in x and y directions. The domain of the cell size was meshed near the stem by about 1 mm and the largest cell size has limited as 10 mm. The total numbers of cells are shown in Table 1 and the mesh is shown in Figure2. The values of the main variables in the simulations are gathered in Table 1. The values of the main variables in the simulations are summarized in Table 1.

Table 1. Mesh Information

Domain	Nodes	Elements
Fluid	254298	166310

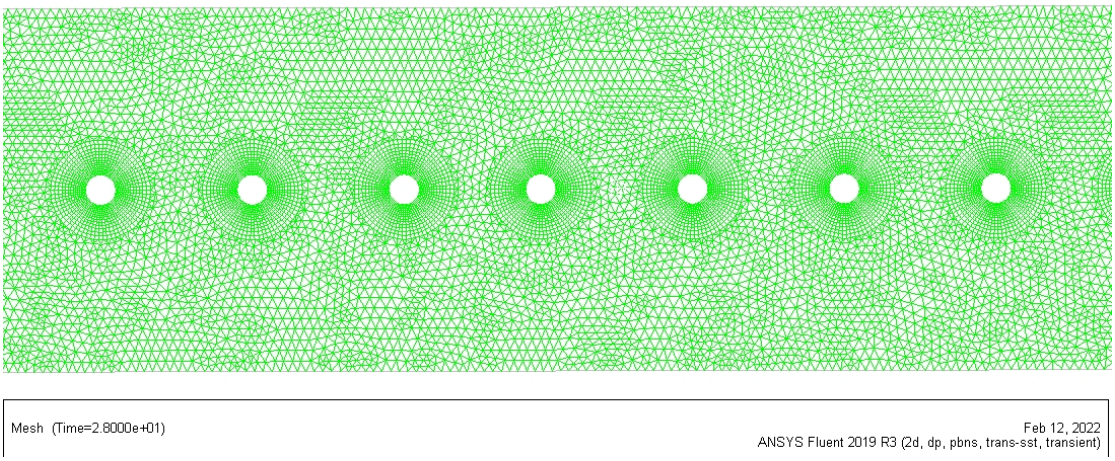

Figure 2. The computational mesh for the in-line circular cylinders of equal diameters.

2.4 Boundary Conditions

Applying the boundary conditions and some important parameters to the numerical model can directly affect the calibration of results. After the validation of numerical results conformity percentage with the experimental results, the values of the parameters that are comparison were applied in the simulation. The boundary conditions used in this study are shown in Table 2. In this model, the specific velocity represents the inlet type of the boundary set at the inlet, while at the outlet, the pressure outlet was set as the boundary. Symmetric boundaries were set at the top and wall boundary at the bottom of the numerical model. These numerical boundaries conditions model is correspond to the physical conditions of the problem.

Table 2. Boundary Physics

Domain	Boundaries	
surface_body	**Boundary - inlet**	
	Type	VELOCITY-INLET
	Boundary - outlet	
	Type	PRESSURE-OUTLET
	Boundary - symmetry 1	
	Type	SYMMETRY
	Boundary - symmetry 2	
	Type	SYMMETRY
	Boundary - wall_channel	
	Type	WALL
	Boundary - wall_cylinder	
	Type	WALL

3 RESUTS

3.1 Velocity Distribution around One-Line Cylinders

Figures 3(a-c) show the time-averaged steady stream-wise velocity distributions associated with a uniform flow pass an array of in-line cylinders of equal diameters. Three spacing ratios (S/D = 10, 5, and 2.5) corresponding to three different circular cylinders (D = 1.25, 2.5, 5.0cm) were examined as case A, B and C. For the small size cylinders (D=1.25 cm), the stream-wise velocity distribution showed a smooth passage of the streamlines, while for the medium cylinder size (D = 2.5 cm) the velocity profiles have affected by the decreasing S/D ratio due to an increase in the cylinder diameter. However, for the largest cylinder diameter (D = 5.0 cm) the velocity distribution has been affected by the decreasing S/D ratio as a result of increasing the cylindrical diameter. It is obvious from these Figures that the velocity distribution for the S/D ratio equal to 5 having different values in comparison to the smallest circular cylinder diameter (D = 1.25 cm) or of spacing ratio S/D = 10.

However, for the largest cylinder diameters (D = 5.0 cm, of S/D = 2.5), the velocity distribution showed an observable suppress of the streamlines due to the small gap between the adjacent cylinders. Positive values of the time-averaged stream-wise velocity depict convection of the coherent structures in the downstream direction of the flow.

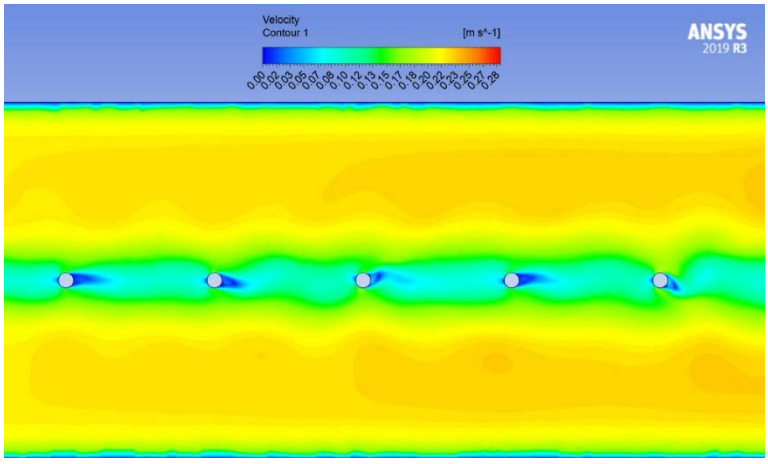

(a)

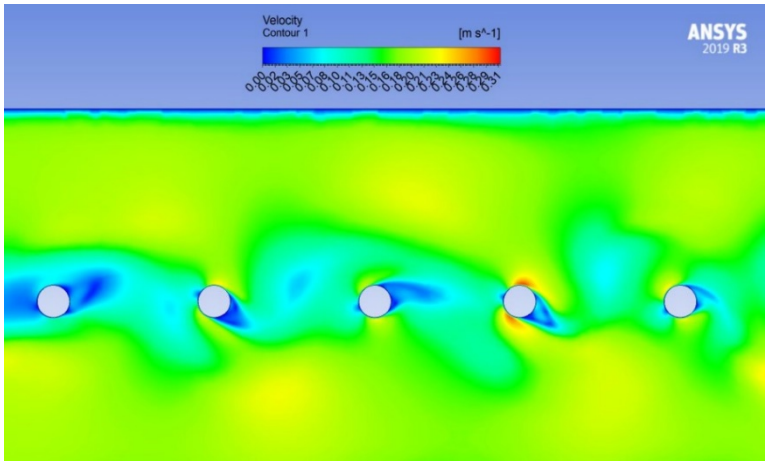

(b)

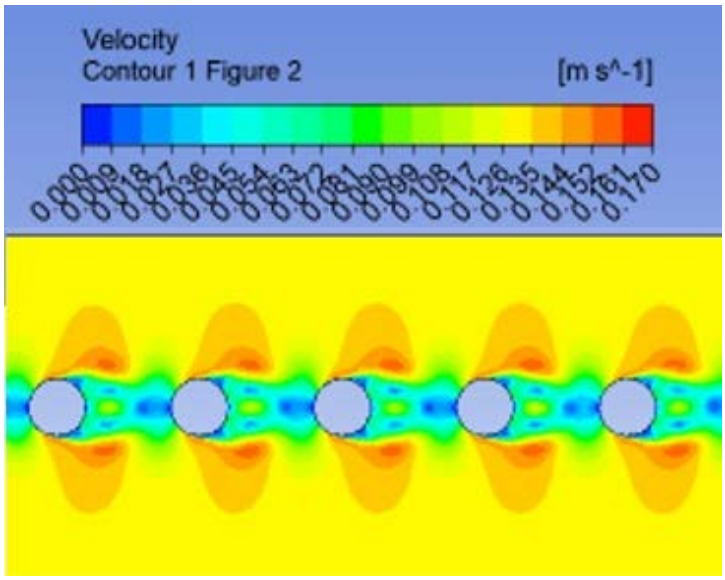

(c)

Figure 3. 2-D time-averaged stream-wise velocity distributions of an in-line circular cylinders

(a) D = 1.25 cm (b) D = 2.5 cm (c) D = 5.0 cm.

3.2 Pressure Fields in Front and Behind the In-Line Cylinders

The time-averaged pressure fields distribution in the vicinity of an array of an in-line cylinders are shown in Figures 4 (a-c). When the flow approaches the stagnation point, high pressure zone in front of the upstream cylinder was recognized. Then the flow is accelerated around the upstream cylinder in the area between the channel wall and the side faces of the cylinder. A steep drop of the pressure will take place. Positive pressure distribution occurs in front of the stagnation point. While, negative values were found at the downstream direction behind the cylinder. The negative values of the pressure were extended far downstream which illustrates prominent vortex shedding as can be seen in Figure 4 a & b for the small and medium cylinder diameters (D = 1.25 cm, 2.5 cm).

For the cylinder diameter D = 5.0 cm, negative values of pressure were extended at smaller distances behind the cylinders (see Figure 4.c). The asymmetric pressure fields in the wake behind the upstream cylinder is due to the vortex shedding pressure presence. (See Figure 4. a & b). However, for the large size cylinder (D = 5.0 cm or S/D = 2.5), symmetric pressure field distribution was observed (Figure 4.c). Thence forward with the flow direction, the pressure zone in front of the upstream cylinder dwindles.

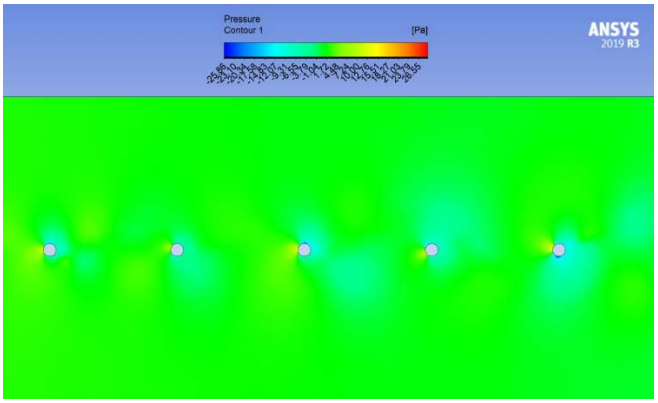

(a)

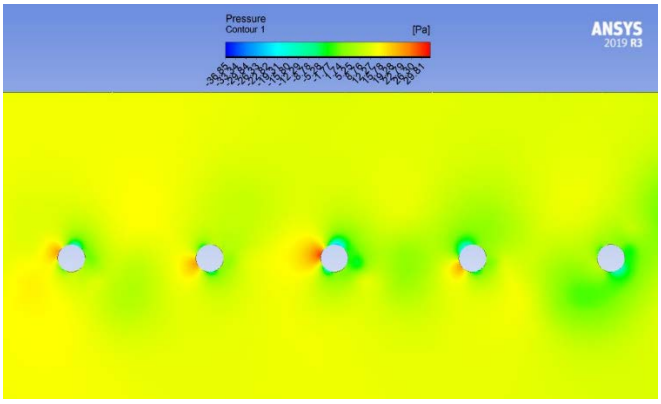

(b)

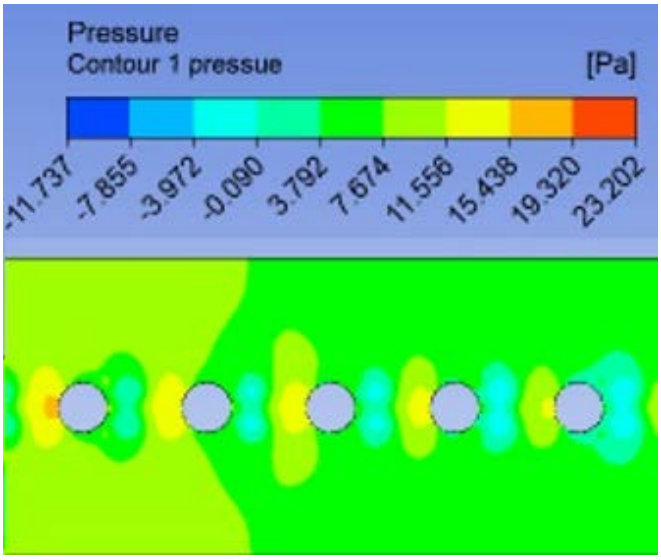

(c)

Figure 4. 2-D time-averaged pressure distributions of an in-line circular cylinders

(a) D = 1.25 cm (b) D = 2.5 cm (c) D = 5.0 cm.

3.3 Time Averaged Turbulent Kinetic Energy

The computed distribution of the time-averaged Turbulent Kinetic Energy (TKE) is shown in Figures. 5 (a-c). The most effected zones of (TKE) can be observed in the gap region and in the wake of the downstream cylinder due to the velocity fluctuations in the x-y directions. High levels of the two-dimensional TKE occurs immediately in front of the downstream cylinders of the large diameter (D = 5.0 cm). However, for medium and small diameters these fluctuations are very small or does not exist.

3.4 Time-Averaged Vorticity

Figures 6 shows the time-averaged vorticity of the numerical simulation of the present work for an array of cylinders in-line configuration. According to the different size of cylinder diameters, two types of flow patterns can be observed around the in-line cylinders. The first pattern is for the cases A and B corresponding to the cylinder diameters of 1.25 cm and 2.5 cm, respectively. The numerical results show that shedding does take place behind the cylinders, which looks like a series of swirls downstream from the cylinders as von Karman vortex street (Figure 6.a & b). In this type, vortex shedding patterns were well predicted in the numerical simulation. The second pattern is for the largest diameters case C, corresponding to cylinder diameter equal to 5.0 cm. In this type the cylinders are close to each other and the flow is suppressed. The flow pattern has characteristic as shear layer reattachment that shear layers separated from both sides of the cylinders. The circulation zones from behind each of the array in-line cylinders, each containing a pair of vortices of equal strength and opposite rotation (Figure 6.c). The recirculation zones are constrained by the cylinders immediately downstream. The numerical results show that the flow pattern is classified as a shear layer reattachment. This situation coincides with the findings of [30] when the cylinders are close to each other with S/D ratio less than 3. In addition, the results showed symmetrical distribution of vortices were captured behind each cylinder and these vortices partially filled the gap between any two cylinders. The numerical simulation performed this very well. Different configurations of vortices distribution behind the cylinders were observed for the cylinder diameters of 1.25 cm and 2.5 cm in comparison to the largest diameter D = 5.0 cm. This difference between the largest cylinder diameter (D = 5 cm) and small diameters (D = 2.5 cm and 1.25 cm) was attributed to the strong interaction of the vortices in the wake of the lined cylinders with the large diameter in comparison to the other diameters.

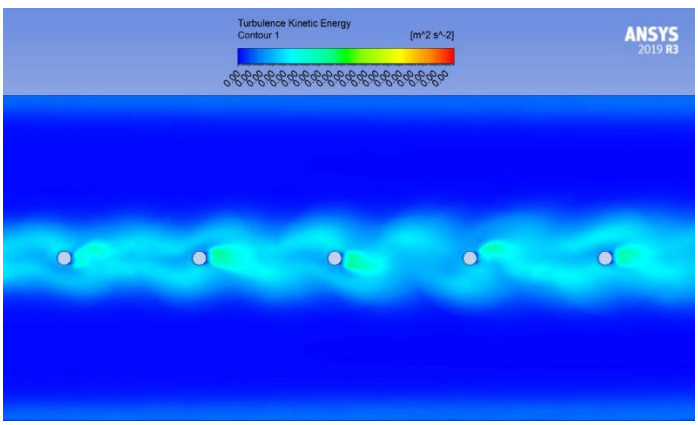

(a)

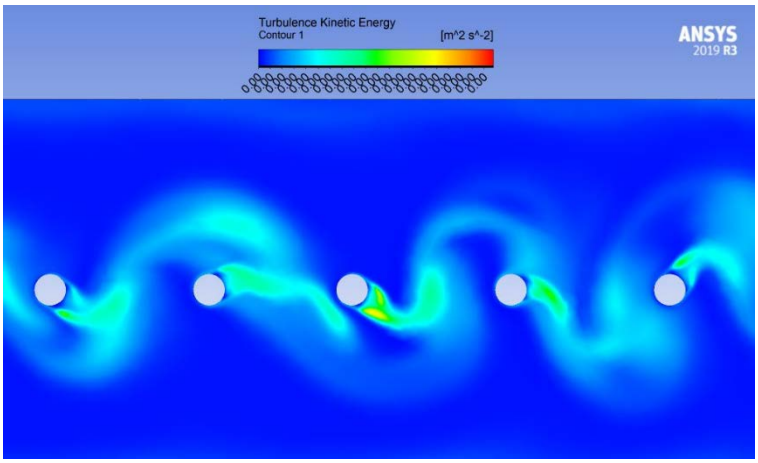

(b)

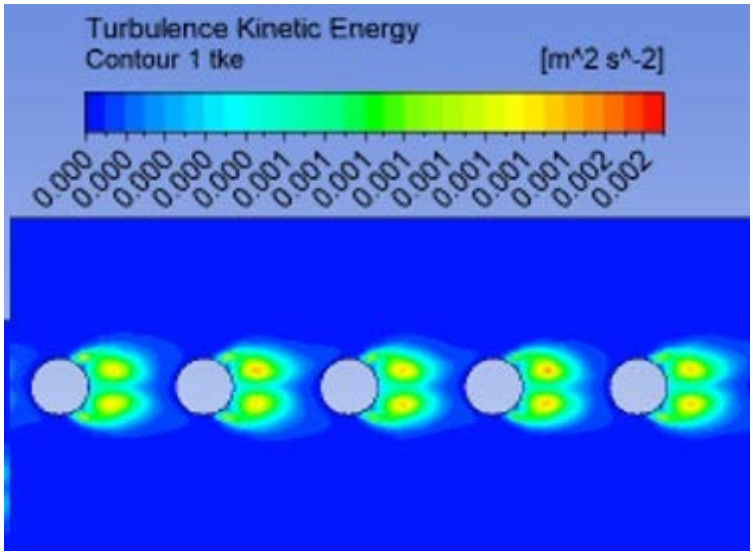

(c)

Figure 5. 2-D time-averaged turbulent kinetic energy distribution of an in-line circular cylinders (a) D = 1.25 cm (b) D = 2.5 cm (c) D = 5.0 cm.

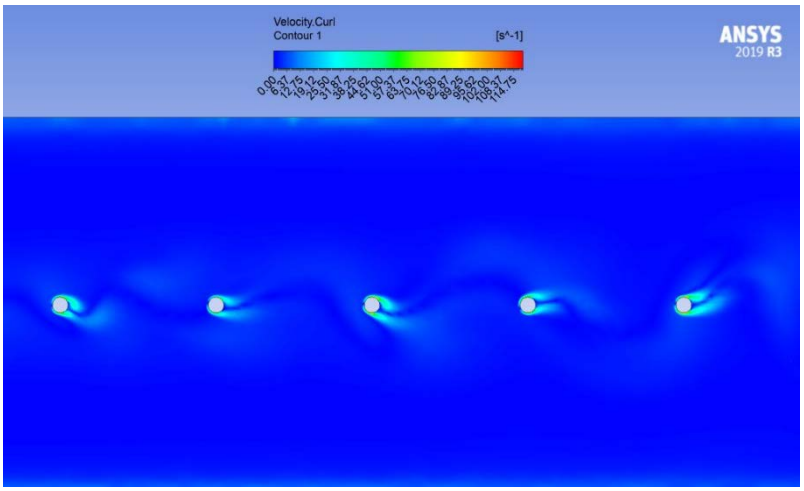

(a)

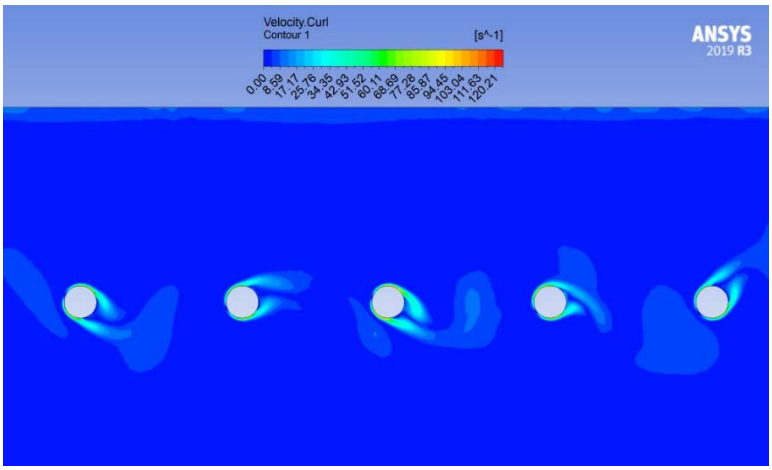

(b)

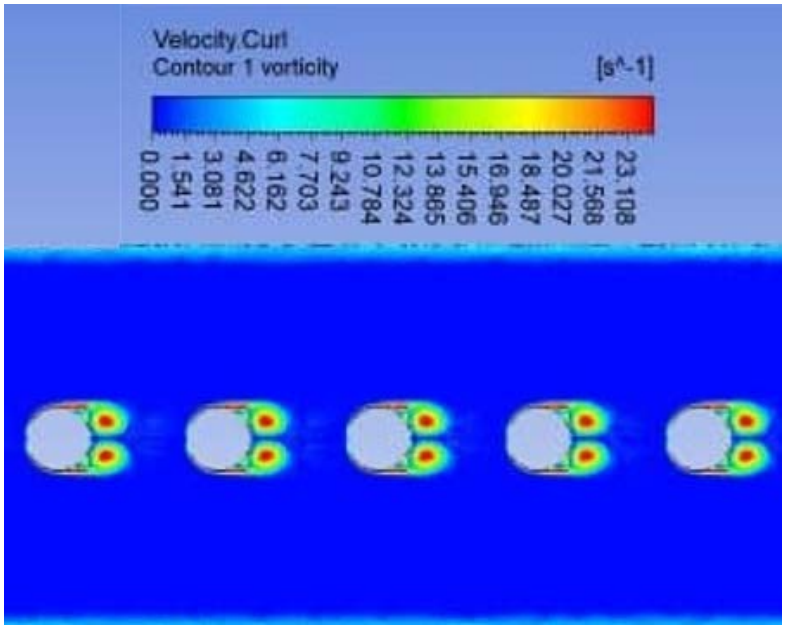

(c)

Figure 6. 2-D time-averaged span-wise vortices distribution of an in-line circular cylinders

(a) D = 1.25 cm (b) d = 2.5 cm (c) d = 5.0 cm.

4 CONCLOUSIONS

The simulation results have demonstrated the capability of CFD to predict the flow properties past a row of circular cylinders located at equispaced distances along the center line of the laboratory channel. Three spacing ratios S/D = 10, 5, and 2.5 corresponding to cylinder diameters 1.25 cm, 2.5 cm and 5.0 cm respectively were examined under uniform flow conditions. The concluded points from the simulation results are as follows:

1) Two distinct flow patterns have been monitored; the shear layer flow patterns and shedding with von Karman Vortex Street.
2) Different velocity profiles were well simulated which are showing the effect of the S/D ratio corresponding to the cylinder diameters. Positive stream-wise velocity depicts convection of the flow patterns in the downstream direction of the flow. As the cylinder diameter is increased that results in spacing ratio S/D decreases, there is an observable suppress of the velocity streamlines.
3) For the diameter (1.25 and 2.5 cm), negative pressure values were extended further downstream the cylinders than the diameter of (5 cm), which illustrates prominent vortex shedding for the cases small and medium cylinder diameters (D = 1.25 cm, 2.5 cm). Symmetric pressure field distribution was monitored for the cylinder diameter (D = 5.0 cm) of spacing ratio S/D = 2.5.
4) High levels of the 2D TKE are observable immediately in front of the downstream cylinders for the large diameter, D = 5.0 cm (S/D = 2.5).
5) The numerical results show that the flow patterns are classified as a shear layer reattachment. This situation coincides with the findings of [30] when the cylinders are close to each other with S/D ratio less than 3.

6) Shedding patterns of vortex were well predicted in the numerical simulation behind the cylinders.
7) The CFD numerical simulation ANSYS is well performed to simulate the different flow patterns through open channels in the vicinity of in-line cylinders.
8) The difference of the low patterns between the largest rod diameter (D = 5 cm) and the small diameters (D = 2.5 cm, and 1.25 cm) was resulted from the strong interaction of the vortices in the wake of the in-line cylinders with large diameter in comparison to the other two diameters.

5 ACKNOWLEDGEMENT

The authors would like to thanks Mustansiriyah University (https://uomustansiriyah.edu.iq/), Baghdad-Iraq for its support in the present work.

6 REFERENCES

[1] Niemann, H. J., & Holscher, N. (1990). A review of recent experiments on flow past circular cylinders. Journal of Wind Engineering and Industrial Aerodynamics, 33(1-2), 197-209, https://doi.org/10.1016/0167-6105(90)90035-B.

[2] Mulahasan S., Stoesser T. and McSherry R. (2017). Effect of floodplain obstructions on the discharge conveyance capacity of compound channels. Journal of Irrigation and Drainage Engineering, 2017, 143(11), https://dx.doi.org/10.1061/(ASCE)IR.1943-4774.00012.

[3] Mulahasan S. (2017). Effect of sidewall proximity on the flow around a circular cylinder. 4th International Symposium on Shallow Flows. Eindhoven University of Technology, NL, 26-28 June.

[4] Zdravkovich, M. M. (1987). The effects of interference between circular cylinders in cross flow. Journal of Fluids and Structures, 1(2), 239-261, https://doi.org/10.1016/S0889-9746(87)90355-0.

[5] Papaioannou, G. V., Yue, D. K., Triantafyllou, M. S., and Karniadakis, G. E. (2006). Three-dimensionality effects in flow around two tandem cylinders. Journal of Fluid Mechanics, 558, pp. 387–413. https://doi.org/10.1017/S0022112006000139.

[6] Lockard, D., Choudhari, M., Khorrami, M., Neuhart, D., Hutcheson, F., Brooks, T., and Stead, D. (2008). Aeroacoustic simulations of tandem cylinders with subcritical spacing. In 14th AIAA/CEAS Aeroacoustics Conference (29th AIAA Aeroacoustics Conference) https://doi.org/10.2514/6.2008-2862.

[7] Palau-Salvador, G., Stoesser, T. and Rodi, W. (2008). LES of the flow around two cylinders in tandem" Journal of Fluids and Structures, 24(8), 1304-1312 https://doi.org/10.1016/j.jfluidstructs.2008.07.002.

[8] Zdravkovich, M. M (1997). Flow around circular cylinders. Volume 2: Applications (Vol 2). Oxford University Press.

[9] Aiba, S. and Yamazaki, Y. (1976). An Experimental investigation of heat transfer around a tube in a bank', Journal of Heat Transfer, 98(3), 503-512, https://doi.org/10.1115/1.3450583.

[10] Igarashi, T. & Suzuki, K. (1984). Characteristics of the flow around three circular cylinders. Bulletin of Japan Socity of Mechanical Engineering, 27, 2397-2404, quoted in M. M. Zdravkovich, Flow around circular cylinders. Volume 2: Applications, 1080, https://doi.org/10.1299/jsme1958.27.2397.

[11] Igarashi, T (1986). Characteristics of the flow around four circular cylinders arranged in- line. Bulletin of Japan Society of Mechanical Engineers, 29, 751-7. Quoted in M.M. Zdravkovich, Flow around circular cylinders Volume 2: Applications, 1097, https://doi.org/10.1299/jsme1958.29.751.

[12] Crowdy, D. G. (2006). Analytical solutions for uniform potential flow past multiple cylinders. European Journal of Mechanics B/Fluids, 25, 459–470.

[13] Fornarelli, F., Oresta, P. and Lippolis, A. (2014). Flow patterns and heat transfer around six in-line circular cylinders at low Reynolds number, https://doi.org/10.17654/JP2015_001_028.

[14] Fornarelli, F., Lippolis, A. and Oresta, P. (2016) Buoyancy induced transitions on heat and mass transfer around multiple bluff bodies. Journal of Heat Transfer, 139 (2), https://doi.org/10.1115/1.4034794.

[15] Liang C., Papadakis, G., Luo, X. (2009). Effect of tube spacing on the vortex shedding characteristics of laminar flow past an inline tube array: A numerical study. Computers & Fluids, 38, 950–964, https://doi.org/10.1016/j.compfluid.2008.10.005.

[16] Mulahasan S. & Stoesser T. (2015). Flow resistance of in-line vegetation in open channel flow. International Journal of River Basin Management, https://doi.org/10.1080/15715124.2017.1307847.

[17] Yokojima, S., Asaoka, R., Yoshino, K., Noda, H. & Miyahara, T. (2017). On permeability and roughness effects in flow past a row of circular cylinders arranged along the centerline of a straight flume. Proceedings of the 37th IAHR World Congress August 13 – 18, 2017, Kuala Lumpur, Malaysia.

[18] Sun, X., and Shiono, K. (2009). Flow resistance of one-line emergent vegetation along the floodplain edge of a compound open channel. Advances in Water Resources, 32, 430–438, https://doi.org/10.1016/j.advwaters.2008.12.004.

[19] Terrier, B. (2010) Flow characteristics in straight compound channels with vegetation along the main 567 channel, Dessertation presented to Department of Civil and Building Engineering 568Loughborough University.

[20] Goliatt, L., Sulaiman, S. O., Khedher, K. M., Aitazaz Ahsan Farooque, A. A., and Yaseen. Z. M. (2021). Estimation of natural streams longitudinal dispersion coefficient using hybrid evolutionary machine learning model. Engineering Applications of Computation Fluid Mechanics, 15, 1298-1320, https://doi.org/10.1080/19942060.2021.1972043.

[21] Zhao, M., Kaja, K., Xiang, Y., and Cheng, L. (2016). Vortex-induced vibration of four cylinders in an in-line square configuration. Physics of Fluids, 28, 023602, https://doi.org/10.1063/1.4941774.

[22] Gubashi, K. R., Mulahasan, S., Jameel, M. A., and Al-Madhhachi, A. S. T. (2022). Evaluation drag coefficients for circular patch vegetation with different riverbed roughness. Cogent Engineering, 9 (1), 2044574, https://doi.org/10.1080/23311916.2022.2044574.

[23] Salvador, G. P., Stoesser, T., Fröhlich, J., and Wolfgang Rodi, W. (2008). LES of the flow around two cylinders in tandem, Journal of Fluids and Structures, 24 (8), 1304-1312, https://doi.org/10.1016/j.jfluidstructs.2008.07.002.

[24] Hamed, A.M., Peterlein, A. M., and Randle, L. V. (2019). Turbulent boundary layer perturbation by two wall-mounted cylindrical roughness elements arranged in tandem: Effects of spacing and height ratio, Physics of Fluids 31, 065110; https://doi.org/10.1063/1.5099493

[25] Keshvarzi, A., Shrestha, C. K., Zahedani, M. R., Ball, J., & Khabbaz, H. (2018). Experimental study of flow structure around two in-line bridge piers. In Proceedings of institution of civil engineers-water management 171, (6), 311-327. Thomas Telford Ltd.

[26] Al-Hashimi, S. AM., Saeed, K. A., and Nahi, T. (2019). Experimental and CFD Modeling of Hydraulic Jumps Forming at Submerged Weir. Journal of The Institution of Engineers (India) Series A, (100), 487-493, https://doi.org/10.1007/s40030-019-00381-z

[27] Launder, B. E. and Sharma, B. I. (1974). Application of the energy dissipation model of turbulence to the calculation of flow near a spinning disc. Letter in Heat and Mass Transfer, 1 (2), 131-137.

[28] Wilcox, D.C. (1998). Turbulence Modeling for CFD. 2nd Edition, DCW Industries, La Canada, California.

[29] Launder, B.E. and Spalding, D.B. (1974). The Numerical computation of turbulent flows. Computer Methods in Applied Mechanics and Engineering, 3, 269-289, https://doi.org/10.1016/B978-0-08-030937-8.50016-7.

[30] Sumner, D., Richards, MD., Akosile, OO. (2005). Two staggered circular cylinders of equal diameter in cross flow. Journal of Fluids and Structures, 20, 255-276, https://doi.org/10.1016/jfluidsstructs.2004.10.006.

Paper submitted: 09.09.2022.

Paper accepted: 27.11.2022.